ACS APPLIED MATERIALS & INTERFACES

RESEARCH ARTICLE

www.acsami.org

Rapid Deposition of Transparent Super-Hydrophobic Layers on Various Surfaces Using Microwave Plasma

Alexander Irzh, Lee Ghindes, and Aharon Gedanken*

Department of Chemistry and Kanbar Laboratory for Nanomaterials at the Bar-Ilan University Center for Advanced Materials and Nanotechnology, Bar-Ilan University, Ramat-Gan, 52900, Israel

Supporting Information

ABSTRACT: We report herein on a very fast and simple process for the fabrication of transparent superhydrophobic surfaces by using microwave (MW) plasma. It was found that the reaction of various organic liquids in MW argon plasma yields hydrophobic polymeric layers on a large assortment of surfaces, including glass, polymeric surfaces, ceramics, metals, and even paper. In most cases, these polymers are deposited as a rough layer composed of 10−15 nm nanoparticles (NPs). This roughness, together with the chemical hydrophobic nature of the coated materials, is responsible for the superhydrophobic nature of the surface. The typical reaction time of the coating procedure was 1−10 s. The stability of these superhydrophobic surfaces was examined outdoors, and was found to last 2−5 days under direct exposure to the environment and to last 2 months when the sample was protected by a quartz cover. A detailed characterization study of the chemical composition of the layers followed using XPS, solid-state NMR, and IR measurements. Modifications were introduced in the products leading to a substantial improvement in the stability of the products outdoors.

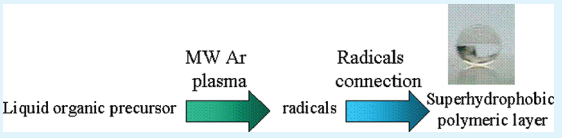

KEYWORDS: superhydrophobic layers, plasma polymerization, coatings, transparency, UV stability, Microwave radiation

1. INTRODUCTION

Over the last years, many papers were published dealing with the preparation of superhydrophobic surfaces.[1−7] It is well-known that to achieve a superhydrophobic surface, two factors have to be fulfilled. The first is a geometric factor, i.e., increasing the surface roughness causes an increase in the hydrophobic property, reaching a superhydrophobic state. The second factor is the surface chemistry, i.e., the superhydrophobic surface has to be composed of hydrophobic moieties. Once the surface is very rough and composed of hydrophobic material, superhydrophobic properties will be detected. The roughness has a distinct effect on the surface behavior, enhancing the wetting properties of the surface. Therefore, a rough hydrophilic surface will become superhydrophilic, as can be seen in the Cassie−Baxter case.[1−4,6] Generally, hydrophobic materials can be divided into three groups. The first one consists of inorganic hydrophobic materials such as ZnO[8−10] or TiO_2.[11] However, these materials lose their hydrophobicity and become superhydrophilic under UV radiation. Superhydrophobicity in such materials can be recovered when the materials are stored in the dark. The second hydrophobic group consists of various hydrocarbons such as polyethylene or polypropylene. The rough layers of these materials are very hydrophobic; however, they undergo oxidation and/or degradation under UV light.[12,13] This is why hydrocarbon-based superhydrophobic materials cannot be used under the ambient conditions of open air. The third group of superhydrophobic materials consists of fluorocarbons such as Teflon. These materials are thermally and UV stable[12] and can be potentially found in various applications such as waterproof clothing, concrete or paint, antirain windshields, materials with very low friction in water (boats or swimsuit coatings, plastics for microfluidics), etc.[3] Unfortunately, the accumulation of contamination, as well as the low wear resistance of these materials, limits their practical use.[3,6] Nevertheless, there is still an increasing demand for superhydrophobic surfaces, which calls for the development of methods for fast, easy, and reproducible production. Many of the methods mentioned in the literature are quite complex and time-consuming, and usually necessitate two synthetic steps. The first is the roughening of the surface (often by the deposition of silica nanoparticles on the surface) and the second is surface hydrophobization. For example, Su et al.[14] produced a superhydrophobic layer by embedding nanosilica on epoxy resin. This process took about 8 h, after which perfluoroalkyltriethoxysilane was bonded to the silica surface for an additional 12 h. Teshima et al.[15] also produced a superhydrophobic surface in two steps, the first being the roughening of the poly(ethylene terephthalate) surface by radio frequency (RF) plasma for 10 min. In the second step the polymeric rough surface was coated using the Chemical Vapor Deposition (CVD) method by fluoroalkylsilane for 5−10 h. Ling et al.[16] prepared a superhydrophobic layer by binding silica nanoparticles to an amino-terminated self-assembled monolayer for several hours and later coated this surface by 1H,1H,2H,2H-perfluorodecyltriethoxysilane (PFTS) under vacuum for 5 h. The authors also sintered the surface at 900−1100 °C for 30−120 min. Bravo et al.[17] obtained a superhydrophobic transparent film on the glass substrate using a layer-by-layer process where silica nanoparticles with different sizes

Received: June 5, 2011
Accepted: November 2, 2011
Published: November 02, 2011

were deposited, calcinated at 550 °C for 4 h, and finally coated by trichloro(1H,1H,2H,2H-perfluorooctyl) silane using CVD for an additional 1 h. Xiu et al.[12] prepared UV and a thermally stable superhydophobic layer by depositing silica particles on a glass surface and spin-coating polybutadiene on it. Finally, the polybutadiene-coated film was exposed to SF_6 plasma for 10 min to obtain a fluorinated film. A similar two-stage strategy was adopted by Ming et al.[18] when raspberry-like silica particles were bonded to an epoxy film and coated by poly(dimethylsiloxane) (PDMS) for surface hydrophobization. One of the fastest productions of the superhydrophobic layers was reported by Wang et al.,[19] where a superhydrophobic surface was obtained in a 40 s photografting of acrylic acid onto high-density polyethylene.

Over the past few years, several superhydrophobic layers were produced using plasma polymerization.[20−24] Potentially, this method could be a good technique for a one-step production of a superhydrophobic layer, because the obtained polymeric layer may be simultaneously rough and hydrophobic when suitable monomers are used. However, a CA of 150° could barely be achieved, and reaching this CA usually requires many coating cycles.[24] An additional study of plasma polymerization leading to superhydrophobic layers was conducted by reacting in a pulsed plasma hexafluorobenzene (C_6F_6) monomer.[25] The typical reaction time in this study was 5 min. Using plasma polymerization, a superhydrophobic carbon nanotube forest was prepared successfully[26] in a three-step procedure. In the first step, a Ni thin film (a catalyst) was deposited on the silicon surface, in the second step the carbon nanotube forest was prepared by reacting acetylene and ammonia in a DC plasma discharge, and in the third step the carbon nanotube forest was coated by poly(tetrafluoroethylene. The polymer was formed by reacting hexafluoropropylene oxide using a chemical vapor deposition process on a hot filament at 500 °C. Hess et al.[27] described a method of superhydrophobic coating by plasma-enhanced chemical vapor deposition. In this paper, cellulose paper was coated by a fluorocarbon superhydrophobic layer by using pentafluoroethane as a precursor that was polymerized in plasma for 2 min. As far as we know, one of the fastest procedures to produce a superhydrophobic layer is the polymerization of hexafluoropropylene in 50 Hz AC-voltage plasma on a SU-8 (photoresist) surface.[28] The process took 45 s. However, this process required the roughening of the SU-8 surface prior to the plasma process.

The current article describes a novel one-step or two short-step method for the production of superhydrophobic layers using MW plasma. The one-step reaction was applied for the production of a transparent superhydrophobic layer that was not very UV-stable or a superhydrophobic UV-stable layer that was not very transparent. The two-step method, that is also very short and easy, was applied for the production of a superhydrophobic transparent and UV-stable layer. Only a few seconds were required to produce these layers via a plasma polymerization mechanism. In comparison to all the above-mentioned processes for the fabrication of superhydrophobic surfaces, our technique is much shorter (the two-step process that requires in total less than one minute, is still shorter than all the other reported techniques). The process was carried out on a large assortment of surfaces, which makes our technique not only very time saving, but also cheap and not "substrate dependent". In addition, all the precursors used in this research were stable, commercially available, and relatively cheap. The layers produced in this study could be potentially used in the electronics industry as anticorrosive protective coatings that are not exposed to direct sunlight, or as protective layers on solar cells when the cells are well protected by a quartz shield.

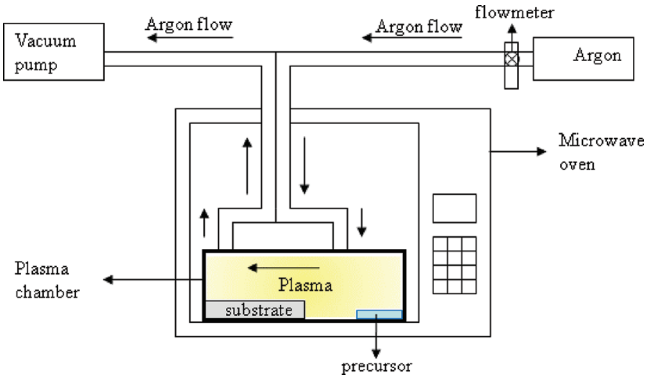

Figure 1. Schematic illustration of the reaction system.

2. EXPERIMENTAL SECTION

Reaction System. The reaction system contains a domestic microwave oven (900W, Crystal) with a drilled hole in its upper part, a plasma chamber made from Pyrex (~5.1 cm wide and ~13.5 cm long), an argon cylinder (99.999%), a vacuum pump (Franklin Electric), and rubber and Pyrex pipes that connect the plasma chamber to the argon cylinder and to the vacuum pump. A schematic illustration of the reaction system is shown at Figure 1.

Coating Procedure. All the reagents were of the highest commercial-available purity, purchased from Aldrich Co., and used without further purification. The glass substrate (25.4 × 76.2 mm, Yancheng Rongkang Glassware Co., Ltd., China, Cat. No. 7102) was inserted into the left side of the plasma chamber. The chamber was loaded by three different precursors, decane (hydrocarbon precursor), TEOS (silane precursor) and perfluorodecaline ($C_{10}F_{18}$) or perfluorononane (C_9F_{20}) (fluorocarbon precursors). In each experiment three drops of decane (~0.018 mL), three drops of TEOS (~0.012 mL), and 15 drops of perfluorodecaline or perfluorodecaline (~0.006 mL) were placed oppositely to the glass slide in the plasma chamber (see Figure 1), and the vacuum pump was activated (the pressure inside the chamber was ~1×10^{-2} Torr). Argon was then pumped through the chamber at a rate of ~50 cc/min for 10 s, after which the microwave oven was activated for 1−5 s. A white glow discharge appeared inside the chamber. At the end of the discharge the glass substrate was coated by a superhydrophobic layer. The overall time of the process was 5 s of the precursor loading +10 s for inserting the substrate into the chamber and connecting/disconnecting the pumps, + 10 s of Ar flowing + up to 5 s of the plasma process ~30 s. The superhydrophobic layers were called by the "p-precursor name", namely, p-TEOS for the layer produced using TEOS, p-decane for the layer produced from decane, p-$C_{10}F_{18}$ for the layer produced from $C_{10}F_{18}$, and p-C_9F_{20} for the layer produced from C_9F_{20}. The thickness of the layers was measured by a profilometer and was found to be 50−70 nm for the p-TEOS layer, while the thickness of the p-C_9F_{20} layer was found to be 40−50 nm. In all cases the thicker part was always closer to the precursor source. In addition, the adhesion of the superhydrophobic layers to the substrates was checked and it was found that they could be removed by simple rubbing. On the other hand, the superhydrophobic layers were not damaged and nor were they removed under a stream of water at the rate of 3 L/min that lasted two minutes. An identical procedure was repeated, coating different substrates such as polycarbonate slides, silicon wafers, aluminum foils, and

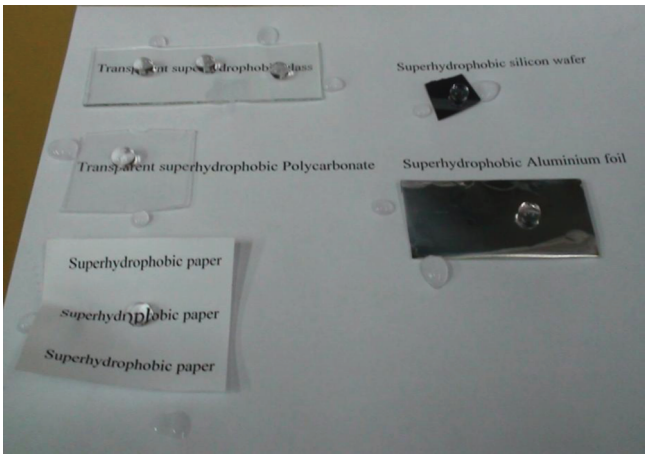

Figure 2. Photograph of water drops on a glass slide, a polycarbonate slide, a silicon wafer, aluminum foil, and paper coated by one thin layer of p-TEOS.

even paper. Superhydrophobic layers were formed on all these substrates (see Figure 2 and the video in Supporting Information).

Characterization Techniques. The thickness of the layers was measured by a Dektak 150 profilometer. The morphology of the prepared surfaces was studied with scanning electron microscopy (SEM) using an Inspect S (FEI Co.) instrument. For higher magnification, the samples were investigated by environmental scanning electron microscopy (ESEM). ESEM imaging was performed using a Quanta 200 FEG (field-emission gun) device. The morphology was also studied by atomic force microscopy (AFM) that was carried out using a Digital Instruments Nanoscope. High-resolution transmission electron microscopy (HRTEM) was measured by a JEOL JEM-2100 electron microscope. The particles were removed from the substrate's surface prior to HRTEM measurements. This was accomplished by scratching the coated upper layer from the glass slide. IR measurements of KBr pellets coated by the investigated superhydrophobic materials were performed by employing an FT-IR Brüker Equinox 55 spectrometer. Coating the product on the KBr pellets was conducted by the MW plasma method. The KBr pellet was introduced into the chamber, replacing the glass slide. The transmittance spectra were recorded on a Cary 100 Scan UV−vis spectrophotometer. Solid-state NMR was recorded on a Bruker 500 Ultra Shield using cross-polarization at ^{13}C and ^{29}Si measurements. An Olympus BX41 (Jobin Yvon Horiba) Raman spectrometer was employed for the produced layer characterization. CA measurements were determined by photographing a drop (~5 μL) of deionized−distilled water placed on the sample with a microsyringe. The surface analysis of the products was conducted by X-ray photoelectron spectroscopy (XPS) on a Kratos Axis HS spectrometer using Al Kα radiation.

3. RESULTS AND DISCUSSION

This paper describes a successful attempt to coat various substrates by superhydrophobic layers within several seconds. The plasma polymerization was adopted as the method for this purpose. As was already reported, organic molecules dissociate in plasma to radicals that are reacting, forming a polymeric network. To check whether our MW plasma system is capable of producing superhydrophobic layers, decane was used as a precursor. It is very logical to assume that polymerized decane (p-decane) will be a hydrophobic polymer, but it was also important to check if the produced layers will also be homogeneous and rough.

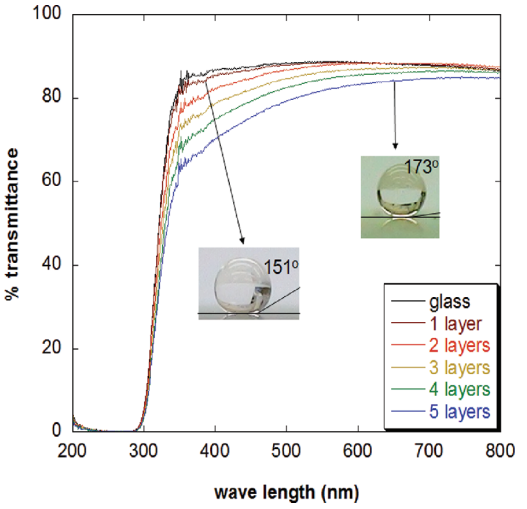

Figure 3. UV−visible spectra of an uncoated glass slide and of glass slides coated by 1−5 layers of p-triethylsilane. The photographs also illustrate water drops placed on glass coated by 1 layer and 5 layers of p-triethylsilane.

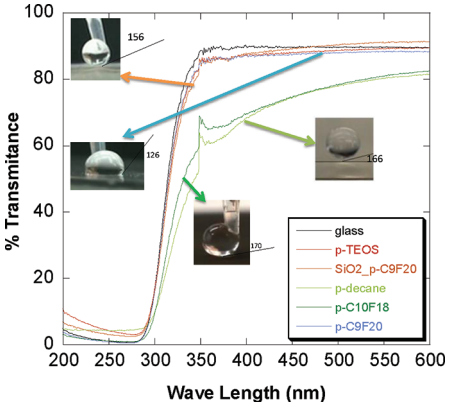

Figure 4. UV−visible spectra of an uncoated glass slide and of glass slides coated by p-TEOS, SiO_2-p-C_9F_{20}, p-decane, p-$C_{10}F_{18}$, and p-C_9F_{20}. The drops of water on these surfaces with the CA are also shown (drops of water on p-TEOS are presented in Figure 3).

Formation of p-Decane. After carrying out the above-described procedure, a superhydrophobic layer of p-decane was formed. However, this layer suffered from two big disadvantages; the first was that the p-decane layer had a relatively low transparency in the visible light region (60−80%), as can be seen in Figure 4. The second disadvantage was the very poor stability of this layer in open air. The initial CA of the p-decane layer immediately after the reaction was 166° with low hysteresis (~5°), but after 24 h of storage in a closed room (in a Petri dish, where it was protected from UV light and dust), the CA was reduced significantly to ~120°. The low stability of the p-decane layer was attributed to the significant amount of double bonds in p-decane that can be easily oxidized, causing a decrease in the CA. To estimate the amount of double bonds, the glass coated by the p-decane layer was placed in a bromine-dichloromethane solution overnight. All double bonds should react easily with bromine during this procedure.[29] Afterward, the brominated p-decane layer was examined by XPS and the amount of bromine atoms on the surface of the layer was found to be 6%. Another reason for

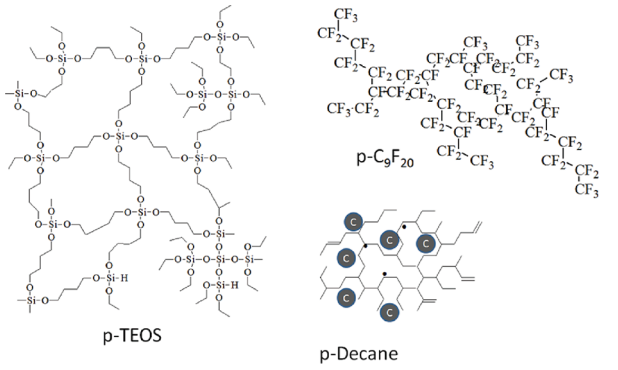

Figure 5. Proposed structure of the various layers (p-TEOS, p-decane, and p-C_9F_{20}) described in this paper.

the low stability of p-decane layers is possibly due to the existence of carbon radicals trapped inside the polymeric matrix in the polymerization process.[30] These radicals undergo oxidation when the layer is exposed to air, and thus the CA is reduced with time. Figure 7a shows the IR spectrum of the p-decane layer. It can be seen that p-decane is composed of only CH_2 and CH_3 groups with a small amount of C═O groups (that were probably formed as a result of C═C oxidation). In addition, the small peak at 3700 cm^{-1} can be attributed to OH groups that were formed as a result of the hydrolysis of C free radicals trapped inside the polymeric matrix, or due to the oxidation of double bonds. On the basis of the IR and XPS spectra, the schematic chemical structure of p-decane is shown at Figure 5.

Formation of p-TEOS. To increase the transparency of the produced superhydrophobic layer, as well as its stability, TEOS was chosen as the precursor. TEOS has a lower percentage of carbon atoms per molecule, and therefore it is logical that p-TEOS will have less double bounds and will therefore show a higher stability. The proposed structure of p-TEOS is depicted in Figure 5, where it can be seen that it is composed of bonded TEOS formed through Si−O−Si bonds. The existence of Si−O−Si bonds and Si−O−R groups (R is a hydrocarbon such as CH_2CH_3) is proved by an IR spectrum shown in Figure 7b. The intense peak at 1070 cm^{-1} is assigned to the siloxane asymmetric-bond stretching of Si−O−Si or Si−O−R groups. The 800 cm^{-1} peak is ascribed to Si−O−Si bonds, and the peak at 2930 cm^{-1} is attributed to the CH_2/CH_3 groups. The peak at 880 cm^{-1} demonstrates the existence of $-OSiCH_3$ groups, as seen in Figure 7b. The evidence for hydrocarbon bridges between Si−O groups (Si−O−$(CH_2)_n$−O−Si) was proved by solid state NMR measurements. To measure p-TEOS by solid-state NMR, we coated a glass slide by at least 20 layers of p-TEOS, producing a thick layer. This layer was then removed from the glass slide and measured by solid-state NMR. During the process of depositing so many p-TEOS layers, some of the material was probably carbonized; therefore, the surface coated by 20 p-TEOS layers was gray and not white. On the other hand, a white color was observed after depositing 5 layers. This carbon was also detected by solid-state C^{13} NMR at 0−90 ppm[31] and overlapped with alkyl groups of p-TEOS. The characterization of p-TEOS by solid state NMR relied on references32−35. For additional information on solid state NMR spectra of p-TEOS, see the Supporting Information (Figure 1S).

The produced p-TEOS layer on the glass slide was superhydrophobic with a CA of 151° and an hysteresis of ∼5°. In addition, the p-TEOS layer was very transparent and with the naked eye looked like uncoated glass (transmittance of ∼86−87% in the visible region). Such a high transparency is sufficient for various optical applications, such as protective layers for solar cells. An AFM image of a p-TEOS layer is seen in Figure 6a, which illustrates that this layer is rough and has a hierarchical morphology, namely a p-TEOS layer composed of ∼200 nm aggregates, each of which is composed of small ∼17 nm nanoparticles. The hierarchical structure increases the layers' roughness (that was measured to be 35 nm), which explains the superhydrophobicity of the coated layer. For comparison, the roughness of the uncoated glass was measured to be only ∼3 nm. We tried to increase the CA by depositing layer upon layer five times. Although the glass coated by five layers of p-TEOS was very hydrophobic with a CA of 173°, the transparency of the glass was reduced to ∼80% in the visible region (see Figure 3) and with the naked eye looked a murky-white. For many optical applications, it is required that the transparency of coated surfaces be decreased by only a few percent (usually not more 5%). Therefore, it will be very difficult to integrate glass with an 80% transparency into optic applications.

The stability of the p-TEOS layer was much higher than the stability of p-decane. Under closed room (in a perti dish) conditions, the CA was reduced to 120° after ∼10 days (unlike 1 day in the case of p-decane). Stability tests were also conducted in sunlight, and the CA of 120° was observed after 3 days of exposure. The experiments were conducted during August when average temperatures were 27−32 °C with very low-temperature deviations, the average relative humidity was 75%, and there was no rain. The length of the day was ∼13 h, whereas that of the night was ∼11 h. When the glass slide coated by p-TEOS was covered with a quartz cover that is transparent for UV light, but protects the glass from the accumulation of contaminants, the CA decreased to ∼120° after 5 days. Like the p-decane, p-TEOS was also brominated and checked by XPS. The amount of bromine atoms on the p-TEOS surface was 1.7%, which is much lower than the amount of bromine in brominated p-decane, and therefore, p-TEOS was much more stable than p-decane. It should be noted that the hydrophobicity of p-TEOS is due to the $-CH_2CH_3$ groups on the surface. Such alkane groups can react relatively easily with •OH radicals when they are exposed to UV irradiation under the sun.[36] This is the reason why p-TEOS, even if it does not contain many double bonds, will eventually undergo oxidation and lose its hydrophobicity.

Formation of p-$C_{10}F_{18}$. To produce a better superhydrophobic layer useful for practical applications that have a longer stability when exposed to outdoor conditions, fluorine atoms should be found as the outer atoms. It is well-known that C−F bonds are much stronger than C−H bonds, and also that C−C bonds in fluorinated molecules are stronger than these bonds in alkanes.[37] Therefore, fluorocarbon-based polymers are known to be UV stable. This is the reason why we used perfluorodecaline ($C_{10}F_{18}$) to produce UV stable superhydrophobic layers. p-$C_{10}F_{18}$ was produced as described in the Experimental Section. The initial CA of the obtained surface was 170° with hysteresis of ∼3° (highest CA for a single deposited layer) and remained almost unchanged when stored under a quartz cover exposed to sunlight for two months (after two months the CA decreased to 160° −165°). Unfortunately, when the p-$C_{10}F_{18}$-coated glass was exposed to direct sunlight, the superhydrophobisity was lost after 5 days (the CA decreased to ∼130°) due to the accumulation of polluting molecules from the air. We tried to clean this

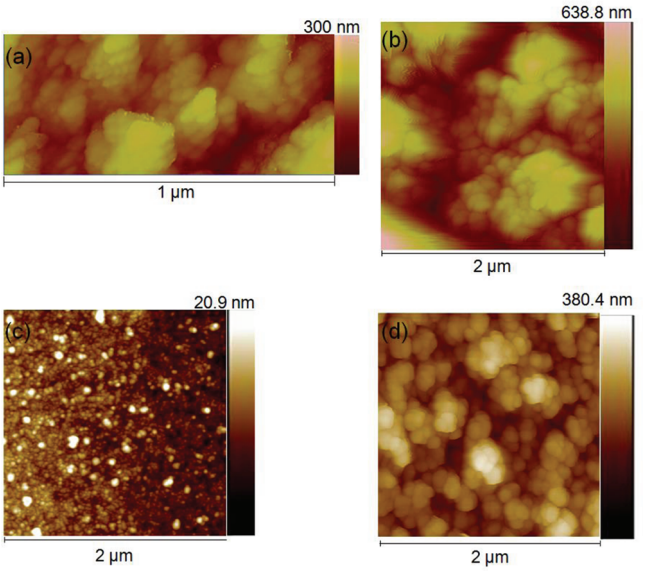

Figure 6. AFM images of glass slides coated by (a) p-TEOS, (b) SiO_2 (annealed p-TEOS in air plasma for 30 s), (c) p-C_9F_{20}, and (d) SiO_2 + p-C_9F_{20}. The roughness of these samples was also measured: (a) 35, (b) 85, (c) 4, and (d) 95 nm.

5-day exposed p-$C_{10}F_{18}$ layer with acetone and ethanol in order to remove the absorbed contamination. Unfortunately, after dipping the sample in acetone and ethanol for 5 min and then drying, the CA did not increase at all and the superhydrophobicity was never recovered.

Another disadvantage of p-$C_{10}F_{18}$-coated glass was that it showed a relatively low transparency in the visible region (60−80%), as shown in Figure 4. Actually, p-$C_{10}F_{18}$-coated glass is brown in color, resembling visually the coating that was obtained with p-decane. This brown color is probably due to the formation of a small amount of carbon, doped inside the polymeric matrix. This carbon can be formed mainly from tertiary carbons in perfluorodecalin, because C−C bonds are weaker than C−F bonds, and therefore tertiary carbons are more likely to be the source of FC or/and C radicals that can combine in the gas phase to carbon- or/and fluorine-doped carbon particles. An additional reason for the brown color could be the light scattering from the rough surface of the p-$C_{10}F_{18}$. XPS measurements were carried out on p-$C_{10}F_{18}$ before and after bromination. An XPS spectrum before bromination is depicted in Figure S2 in the Supporting Information. Figure 2S shows several C1 peaks, such as $-CF_3$ at 292.9 eV, $-CF_2-$ at 290.8 eV, tertiary CF carbon at 288.5 eV, quaternary carbon with neighboring F atoms bonded to carbons ($-CF_n$) at 286.7 eV, as well as an elementary carbon peak (C−C) at 285 eV. The peak at 285.8 eV can be associated with carbon having distanced CF_n neighbor ($\underline{C}-C-CF_n$) in fluorine-doped carbon, but this assignment is speculative. Figure S2 also shows the proposed chemical structure of p-$C_{10}F_{18}$ based on the XPS spectrum. After the bromination, the amount of detected bromine atoms was only 0.2% in the p-$C_{10}F_{18}$ sample, indicating a negligible amount of C═C double bonds.

Formation of p-C_9F_{20} and SiO_2+p-C_9F_{20}. To reduce the amount of doped carbon (and to increase the transparency), we used a linear molecule, perfluorononane (C_9F_{20}), as the precursor. The p-C_9F_{20} layer was indeed very transparent (87−90%

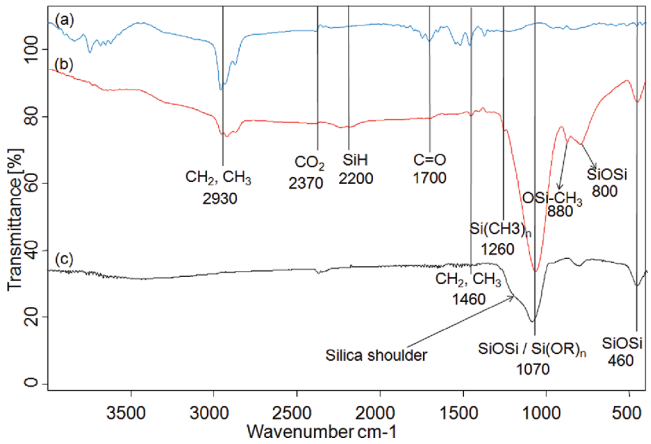

Figure 7. IR spectra of (a) p-decane, (b) p-TEOS, and (c) SiO_2 layer produced after treating p-TEOS in air plasma for 30 s.

in the visible region), although its CA was only ∼126° and it was not superhydrophobic (see Figure 4). The reason for the relatively low CA was because the p-C_9F_{20} coating was very smooth. As is shown in Figure 6c, the p-C_9F_{20} layer is composed of very homogeneous 23 ± 9 nm sized nanoparticles that form a smooth layer on the glass surface with a roughness of only 4 nm (which is very close to the value of the uncoated glass). We believe that the reason for the morphological difference between p-$C_{10}F_{18}$ (rough layer) and C_9F_{20} (smooth layer) is due to the differences between the vapor pressures of the precursors. $C_{10}F_{18}$ is less volatile (having a b.p of 142 °C), and therefore will evaporate more slowly to the gas phase when the vacuum is activated. It allows the reaction of more $C_{10}F_{18}$ molecules via the plasma polymerization process with a lower loss of material. Therefore, in this case the produced layer will be thicker and rougher. On the other hand, C_9F_{18} is more volatile (b.p 125 °C). Therefore, it will evaporate faster when the vacuum is activated, causing a major loss of the material and producing a thinner and a more smooth layer. We tried to enlarge the amount of C_9F_{18} by loading the reactor with more drops. However, we could not activate the plasma as a result of the high pressure inside the chamber. To solve the problem of plasma activation at high pressure, a more powerful MW oven was used (1200 W). In this experiment, loading 30 drops of C_9F_{18} into the chamber enabled the achievement plasma and the production of a deposition. The produced p-C_9F_{18} layer in this case was almost identical to p-$C_{10}F_{18}$, namely, it was superhydrophobic, but brown in color. As with p-$C_{10}F_{18}$, the brown color could have originated from carbon impurities resulting from the possible carbonization of the molecule under such a powerful plasma, or could appear because of the light scattering from the rough surface. To enlarge the roughness of p-C_9F_{18} that was produced by 900 W MW, the glass was coated by a p-TEOS layer on which a p-C_9F_{20} layer was deposited. The deposited p-TEOS layer was exposed to MW plasma under air for 30 s before the deposition of p-C_9F_{20}. In this process, the p-TEOS was decomposed and a rough silica nanolayer was obtained. The IR spectrum of the formed silica layer is shown in Figure 7c. The IR spectrum of silica is similar to the IR spectrum of p-TEOS (Figure 7b), but the typical CH_2, CH_3 peaks at 2930 cm^{-1} are absent. In addition, Figure 7c reveals a typical shoulder of silica at 1200 cm^{-1}. The AFM image of the SiO_2 layer shown in Figure 6b depicts a similar layer to p-TEOS, although, the size of the particles was increased to 87 ± 24 nm.

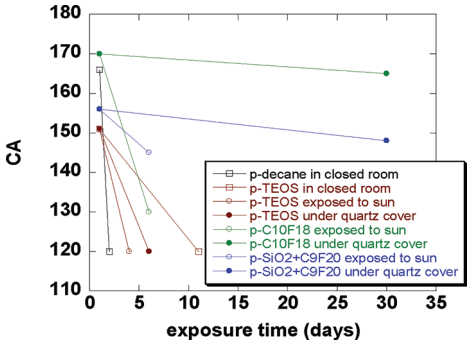

Figure 8. CA change of glass slides coated by various superhydrophobic layers as a function of exposure time under different conditions (e.g., in a closed room where they are protected from UV irradiation and relatively protected from the pollution, exposed to direct sunlight, and exposed to the sun but under a quartz cover that protects the sample from pollution).

This layer was superhydrophilic with a CA of ~0°. The silica-coated glass was then coated by p-C_9F_{20}. The CA of the p-C_9F_{20}-coated silica layer reached ~156° with an hysteresis of ~5° and was superhydrophobic. Figure 6c presents the AFM image of this sample, and also shows that the SiO_2+p-C_9F_{20} layer is composed of 90 ± 23 nm-sized particles forming a very rough layer. The measured roughness of this layer was 95 nm, which is even larger than the measured roughness of p-TEOS. The obtained layer, as depicted in Figure 4, was transparent in the visible region (87−91%, the most transparent superhydrophobic layer produced in this research), and was also as stable as the p-$C_{10}F_{22}$ layer. Superhydrophobicity was detected for five days when it was exposed directly to the sun. It was superhydrophobic for two months when it was covered by a quartz cap. Figure 8 shows the change in the CA of glass coated by the superhydrophobic layers investigated in this research as a function of time. It should be noted that the p-$C_{10}F_{18}$ and SiO_2 + p-C_9F_{20} layers also show a moderate decrease in the CA with time. The CA of SiO_2 + p-C_9F_{20} layer was decreased to 148° after 1 month of the exposure to the sun under quartz cover (see Figure 8). This probably happened because the quartz cover did not protect the sample hermetically, and therefore the accumulation of contamination on the samples was just inhibited, but not totally prevented. The existence of free carbon radicals trapped inside the polymeric matrix that could be responsible for the CA reduction, was examined by ESR measurements. However, we could not detect any ESR signal. The ESR measurements were conducted by dissolving the coated material in distilled water with 5,5-dimethyl-pyrroline N-oxide (DMPO) as a spin trap and also directly by measuring the powder of the coated material.

4. CONCLUSIONS

This article presents a one-step method to produce transparent superhydrophobic layers on a large assortment of surfaces within only a few seconds. By using different precursors, it is possible to design layers with unique properties, such as UV stability and transparency. The most UV stable and most transparent layer was silica-coated glass further coated by a layer of p-C_9F_{20}. The most UV unstable and less transparent layer was glass coated by p-decane. Glass coated by p-$C_{10}F_{18}$ was UV stable (like p-C_9F_{20}) and shows the highest superhydrophobicity (CA = 170°), but demonstrates a relatively low transparency. On the other hand, glass coated by p-TEOS was very transparent but not highly UV stable. In addition, it was found that a layer by layer deposition of p-TEOS increased the CA (up to 173° in the case of 5 layers), but the transparency was decreased.

■ ASSOCIATED CONTENT

Supporting Information. XPS spectra; solid-state NMR spectra; the proposed mechanisms of the MW plasma reactions. This material is available free of charge via the Internet at http://pubs.acs.org.

■ AUTHOR INFORMATION

Corresponding Author
*E-mail: gedanken@mail.biu.ac.il.

■ REFERENCES

(1) Quéré, D. *Annu. Rev. Mater. Res.* **2008**, *38*, 71.
(2) Quéré, D. *Rep. Prog. Phys.* **2005**, *68*, 2495.
(3) Callies, M.; Quéré, D. *Soft Matter* **2005**, *1*, 55.
(4) Feng, X.; Jiang, L. *Adv. Mater.* **2006**, *18*, 3063.
(5) Ma, M.; Hill, R. M. *Curr. Opin. Colloid Interface Sci.* **2006**, *11*, 193.
(6) Li, X.-M.; Reinhoudt, D.; Crego-Calama, M. *Chem. Soc. Rev.* **2007**, *36*, 1350.
(7) Guo, Z.; Liu, W.; Su, B.-L. *J. Colloid Interface Sci.* **2011**, *353*, 335.
(8) Feng, X.; Feng, L.; Jin, M.; Zhai, J.; Jiang, L.; Zhu, D. *J. Am. Chem. Soc.* **2004**, *126*, 62.
(9) Liu, H.; Feng, L.; Zhai, J.; Jiang, L.; Zhu, D. *Langmuir* **2004**, *20* 5659.
(10) Papadopoulou, E. L.; Barberoglou, M.; Zorba, V.; Manousaki, A.; Pagkozidis, A.; Stratakis, E.; Fotakis, C. *J. Phys. Chem. C* **2009**, *113* 2891.
(11) Feng, X.; Zhai, J.; Jiang, L. *Angew. Chem., Int. Ed.* **2005**, *44*, 5115.
(12) Xiu, Y.; Hess, D. W.; Wong, C. P. *J. Colloid Interface Sci.* **2008**, *326*, 465.
(13) Kwak, G.; Lee, M.; Yong, K. *Langmuir* **2010**, *26*, 9964.
(14) Su, C.; Li, J.; Geng, H.; Wang, Q.; Chen, Q. *Appl. Surf. Sci.* **2006**, *253*, 2633.
(15) Teshima, K.; Sugimura, H.; Inoue, Y.; Takai, O.; Takano, A. *Appl. Surf. Sci.* **2005**, *244*, 619.
(16) Ling, X. Y.; Phang, I. Y.; Vancso, G. J.; Huskens, J.; Reinhoudt, D. N. *Langmuir* **2009**, *25*, 3260.
(17) Bravo, J.; Zhai, L.; Wu, Z.; Cohen, R. E.; Rubner, M. F. *Langmuir* **2007**, *23*, 7293.
(18) Ming, W.; Wu, D.; van Benthem, R.; de With, G. *Nano Lett.* **2005**, *5*, 2298.
(19) Han, J.; Wang, X.; Wang, H. *J. Coll, Int. Sci.* **2008**, *326*, 360.
(20) Teare, D. O. H.; Spanos, C. G.; Ridley, P.; Kinmond, E. J.; Roucoules, V.; Badyal, J. P. S. *Chem. Mater.* **2002**, *14*, 4566.
(21) Lacroix, L.-M.; Lejeune, M.; Ceriotti, L.; Kormunda, M.; Meziani, T.; Colpo, P.; Rossi, F. *Surf. Sci.* **2005**, *592*, 182.
(22) Martin, T. P.; Lau, K. K. S.; Chan, K.; Mao, Y.; Gupta, M.; O'Shaughnessy, W. S.; Gleason, K. K. *Surf. Coat. Technol.* **2007**, *201* 9400.
(23) Ji, Y.-Y.; Hong, Y.-C.; Lee, S.-H.; Kim, S.-D.; Kim, S. S. *Surf. Coat. Technol.* **2008**, *202*, 5663.
(24) Ji, Y.-Y.; Kim, S.-S.; Kwon, O. P.; Lee, S.-H. *Appl. Surf. Sci.* **2009**, *255*, 4575.
(25) Yang, S. H.; Liu, C.-H.; Hsu, W.-T.; Chen, H. *Surf. Coat. Technol.* **2009**, *203*, 1379.
(26) Lau, K. K. S.; Bico, J.; Teo, K. B. K.; Chhowalla, M.; Amaratunga, G. A. J.; Milne, W. I.; McKinley, G. H.; Gleason, K. K. *Nano Lett.* **2003**, *3*, 1701.
(27) Balu, B.; Breedveld, V.; Hess., D. H. *Langmuir* **2008**, *24*, 4785.

(28) Wagterveld, R. M.; Berendsen, C. W. J.; Bouaidat, S.; Jonsmann, J. *Langmuir* **2006**, *22*, 10904.
(29) Cossi, M.; Maurizio Persico, M.; Tomas, J. *J. Am. Chem. Soc.* **1994**, *116*, 5313.
(30) Agraharam, S.; Hess, D. W.; Kohl, P. A.; Bidstrup Allen, S. *J. Electrochem. Soc.* **2000**, *147*, 2665.
(31) Shin, Y.; Wang, L.-Q.; Bae, I.-T.; Arey, B. W.; Exarhos, G. J. *J. Phys. Chem. C* **2008**, *112*, 14236.
(32) Engelhardt, G.; Jancke, H. *Polym. Bull.* **1981**, *5*, 557.
(33) Glaser, R. H.; Wilkes, G. L. *J. Non-Cryst. Solids* **1989**, *113*, 73.
(34) Chiang, C.-L.; Ma, C.-C.; Wu, D.-L.; Kuan, H.-C. *J. Polym. Sci. part A Polym. Chem.* **2003**, *41*, 905.
(35) Albert, K.; Bayer, E. *J. Chromatogr.* **1991**, *544*, 345.
(36) Atkinson, R. *Atmos. Environ.* **2000**, *34*, 2063.
(37) Luo, Y.-R. *Comprehensive Handbook of Chemical Bond Energies*; CRC Press: Boca Raton, FL, 2007.